Chapter

Significant Role of Perovskite Materials for Degradation of Organic Pollutants

Someshwar Pola and Ramesh Gade

Abstract

The advancement and the use of visible energy in ecological reparation and photodegradation of organic pollutants are being extensively investigated worldwide. Through the last two decades, great exertions have been dedicated to emerging innocuous, economical, well-organized and photostable photocatalysts for ecofriendly reparation. So far, many photocatalysts mostly based on ternary metal oxides and doped with nonmetals and metals with various systems and structures have been described. Among them, perovskite materials and their analogs (layer-type perovskites) include an emerged as semiconductor-based photocatalysts due to their flexibility and simple synthesis processes. This book chapter precisely concentrates on the overall of related perovskite materials and their associated systems; precisely on the current progress of perovskites that acts as photocatalysts and ecofriendly reparation; explores the synthesis methods and morphologies of perovskite materials; and reveals the significant tasks and outlooks on the investigation of perovskite photocatalytic applications.

Keywords: layered-type perovskite materials, photocatalysis, photodegradation, organic pollutants

1. Introduction

Solar energy is one of the primary sources in the field of green and pure energy that points to the power predicament and climate change task. Solar energy consumption is an ecological reconciliation, and then, the chemical change in solar is presence exhaustive, considered throughout global [1, 2]. In general, solar energy is renewed into a wide range of developments, such as degradation of organic pollutants as photocatalysis, splitting of water molecules for producing clean energy, and reduction of CO_2 gas [3, 4]. Consuming a similar perception, metal-oxide photocatalysis has also been widely examined for possible exertions in ecological restitution as well as the photodegradation and elimination of organic toxins in the aquatic system [5, 6], decrease of bacterial inactivation [7–9], and heavy metal ions [10–12]. Throughout the earlier few years, excellent applications have been dedicated to evolving well-organized, less expensive, and substantial photocatalysts, particularly those that can become active under visible light such as $NaLaTiO_6$, $Ag_3PO_4/BaTiO_3$, $Pt/SrTiO_3$, $SrTiO_3$-TiN, noble-metal-$SrTiO_3$ composites, $GdCoO_3$, orthorhombic perovskites $LnVO_3$ and $Ln_{1-x}Ti_xVO_3$ (Ln = Ce, Pr, and Nd), $Ca_{0.6}Ho_{0.4}MnO_3$, Ce-doped $BaTiO_3$, fluorinated Bi_2WO_6, graphitic

carbon nitride-Bi_2WO_6, $BaZrO_{3-\delta}$, $CaCu_3Ti_4O_{12}$, [13–24], graphene-doped perovskite materials, and nonmetal-doped perovskites [25]. Furthermore, directed to years extended exhaustive investigation exertions on the pursuit of innovative photocatalytic systems, particularly that can produce the overall spectrum of visible-light. Out of a vast assemblage of photocatalysts, perovskite or layered-type perovskite systems and its analogs include a better candidate for capable semiconductor-based photocatalysts due to their framework easiness and versatility, excellent photostability, and systematic photocatalytic nature. In general, the ideal perovskite structure is cubic, and the formula is ABO_3. Where A is different metal cations having charge +1 or +2 or +3 nature and B site occupies with tri or tetra and pentavalent nature, which covers the whole family of perovskite oxide materials by sensibly various metal ions at A and B locations [26], aside from a perfect cubic perovskite system, basic alteration perhaps persuaded by several cations exchange. Such framework alteration could undoubtedly vary the photophysical, optical, and photocatalytic activities of primary oxides.

Moreover, a sequence of layered-type perovskite materials contains many 2D blocks of the ABO_3 framework, which are parted by fixed blocks. The scope of formulating multicomponent perovskite systems by whichever fractional change of cations in A and B or both positions or injecting perovskite oxides into a layered-type framework agrees scientists investigate and control the framework of crystals and the correlated electronic and photocatalytic activities of the perovskites. So far, hundreds of various types of perovskite or perovskite-based catalysts have been published, and more outstandingly, some ABO_3-related materials became renowned with "referred" accomplishment for catalytic activities. Thus, these systems (perovskite materials) have exposed highly capable of upcoming applications on the source of applying more attempts to them. While several outstanding reviews mean that explained that perovskites performed as photocatalyst for degradation of organic pollutants [27–30], only an insufficient of them content consideration to inorganic perovskite (mostly ABO_3-related) photocatalysts [31–33]. A wide range of tagging and complete attention of perovskite materials, for example, layered-type perovskite acting as photocatalysts, is relatively deficient. The purpose of this book chapter is to precise the current progress of perovskite-based photocatalysts for ecological reparation, deliberate current results, and development on perovskite oxides as catalysts, and allow a view on the upcoming investigation of perovskite materials. After a short outline on the wide-ranging structure of perovskite oxides, it was stated that perovskites act as a photocatalyst that are incorporated, arranged and explored based on preparation methods [29, 34], photophysical properties based on bandgap energies, morphology-based framework and the photocatalytic activities depends on either UV or visible light energy of the semiconducting materials. Finally, this chapter is based on the current advancement and expansion of perovskite photocatalytic applications under solar energy consumption. The potential utilization, new tasks, and the research pathway will be accounted for the final part of the chapter [35].

2. Results and discussion

2.1 Details of perovskite oxide materials

2.1.1 Perovskite frameworks

The standard system of perovskite-based materials could be designated as ABO_3, where the A and B are cations with 12-fold coordinated and 6-fold

coordinated to concerning oxygen anions. **Figure 1a** describes the typically coordinated basic of the ABO_3 system, which consists of a 3D system, BO_6 octahedra as located at corner, and at the center, A cation are occupied. Within the ABO_3 system, the A cation usually is group I and II or a lanthanide metal, whereas the B is commonly a transition metal ion. The tolerance factor (t) = 1 calculated by using an equation $t = (rA + rO)/\sqrt{2}\,(rB + rO)$, where r_O, r_A, and r_B are the radii of respective ions A and B and oxygen elements for a cubic crystal structure ABO_3 perovskite system [36].

For constituting a stable perovskite, it is typically the range of t value present in between 0.75 and 1.0. The lower value of t builds a somewhat slanted perovskite framework with rhombohedral or orthorhombic symmetry. In the case of t, it is approximately 1; then, perovskite structure is an ideal cubic system at high temperatures. Even though the value of t, obtained by the size of metal ion, is a significant guide for the permanency of perovskite systems, the factor of octahedral (u) $u = r_B/r_O$ and the role of the metal ions composition of A and B atoms and the coordination number of respective metals are considered [37]. Given the account of those manipulating factors and the electro-neutrality, the ABO_3 perovskite can hold a broad variety of sets of A and B by equal or dissimilar oxidation states and ionic radii. Moreover, the replacement of A or B as well as both the cations could be partly by the doping of various elements, to range the ABO_3 perovskite into a wide-ranging family of $A^1_m A^1_{1-m} B^1_n B^1_{1-n} O_{3\pm\delta}$ [38]. The replacement of several cations into the either A or B positions could modify the structure of the original system and therefore improve the photocatalytic activities [23]. After various metal ions in perovskite oxide are doped, the optical and electronic band positions, which influence the high impact on the photocatalytic process, are modified [24].

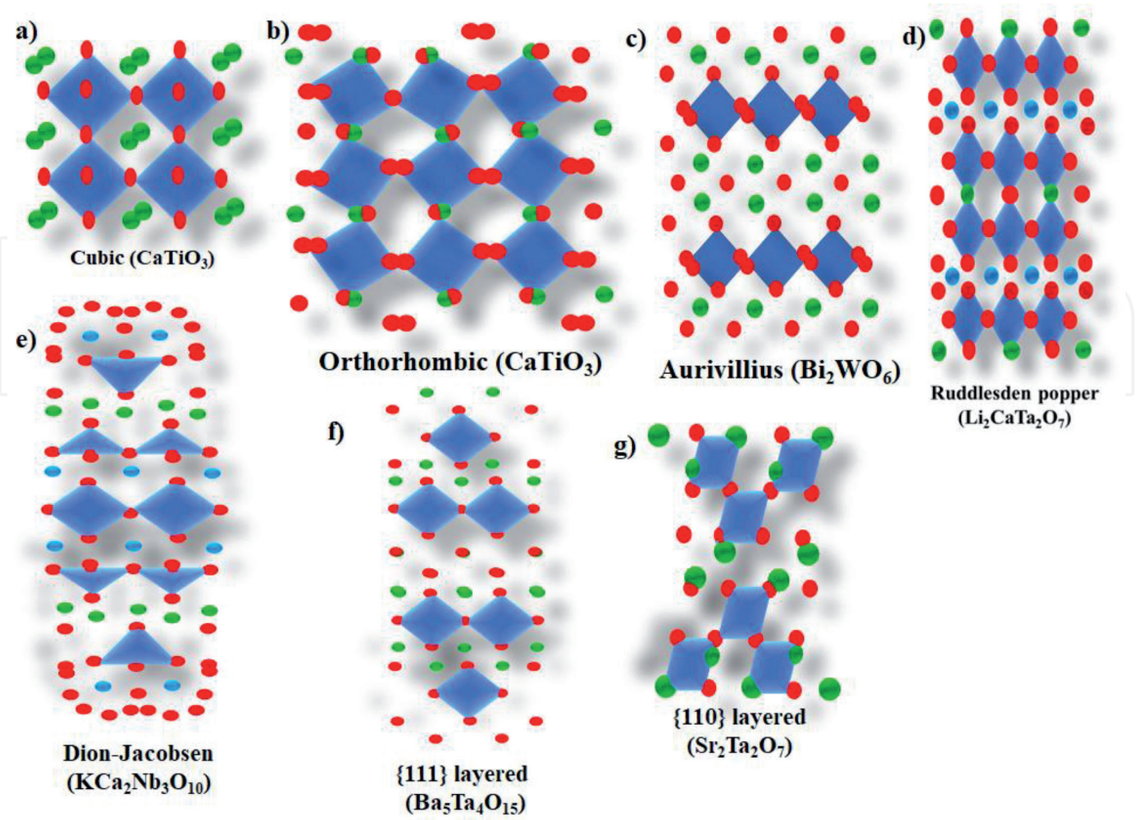

Figure 1.
Both crystal and layered type perovskite oxides (blue small balls: A-site element; dark blue squares: BO_6 octahedra with green and red balls are oxygen).

2.1.2 Layered perovskite-related systems

Moreover, to the overall ABO_3 system, further characteristic polymorphs of the perovskite system are Brownmillerite (BM) ($A_2B_2O_5$) framework [39]. BM is a type of oxygen-deficient perovskite, in which the unit cell is a system of well-organized BO_4 and BO_6 units. The coordination number of cations occupied by A-site was decreased to eight because of the oxygen deficiency. Perovskite (ABO_3) oxides have three dissimilar ionic groups, construction for varied and possibly useful imperfection chemistry. Moreover, the partial replacement of A and B ions is permitted even though conserving the perovskite system and shortages of cations at the A-site or of oxygen anions are common [40]. The Ion-exchange method is used for the replacement of existing metal ions with similar sized or dissimilar oxidation states; then, imperfections can be announced into the system. The imperfection concentrations of perovskites could be led by doping of different cations [24]. Oxygen ion interstitials or vacancies could be formed by the replacement of B-position cations with higher or lower valence, respectively, fabricating new compounds of $AB_{(1-m)}B_m^{I}O_{3-\delta}$ [41]. A typical oxygen-deficient perovskite system is Brownmillerite ($A_2B_2O_5$), in which one part of six oxygen atoms is eliminated. Moreover, the replacement of exciting a site cation to new cation with higher oxidation state metal ions then the formed new materials with new framework with different stoichiometry is $A_{1-m}A_m^{I}BO_3$ [41]. In the case of the replacement of A-site ions with smaller oxidation state cations, consequences in oxygen-deficient materials with new framework such as $A_{1-m}A_m^{I}BO_{3-x}$ are developed. Thermodynamically, the replacement of B-position vacancies in perovskite systems is not preferable due to the compact size and the high charge of B cations [42]. A-position vacancies are more detected due to the BO_3 range in perovskite system forms a stable network [43]; the 12 coordinated sites can be partly absent due to bigger-size A cations. Lately, presenting suitable imperfections on top of the surface of perovskite oxides has been thoroughly examined as a means of varying the bands' position and optical properties of the starting materials. For this reason, perovskite materials afford a tremendous objective for imperfection originating to vary the photocatalytic activity of perovskite material-based photocatalysts [44].

The typical formula for the furthermost recognized layered perovskite materials is designated as $A_{n+1}B_nO_{3n+1}$ or $A_2^{I}A_{n-1}BnO_{3n+1}$ (Ruddlesden-Popper (RP) phase), $A^{I}[A_{n-1}B_nO_{3n+1}]$ (Dion-Jacobson (DJ) phase) for {100} series, ($A_nB_nO_{3n+2}$) for {110} series and ($A_{n+1}B_nO_{3n+3}$) for {111}, and $(Bi_2O_2)(A_{n-1}B_nO_{3n+1})$ (Aurivillius phase) series. In these systems, n represents the number of BO_6 octahedra that duration a layer, which describes the width of the layer. Typical samples of these layered systems are revealed in **Figure 1c–g**. For RP phases, their frameworks consist of $A^{I}O$ as the spacing layer for the intergrowth ABO_3 system. These materials hold fascinating properties such as ferroelectricity, superconductivity, magnetoresistance, and photocatalytic activity. Sr_2SnO_4 and $Li_2CaTa_2O_7$ systems are materials of simple RP kind photocatalysts. A common formula for DJ phase is $A^{I}[A_{n-1}B_nO_{3n+1}]$ (n > 1), where A^{I} splits the perovskite-type slabs and is characteristically a monovalent alkali cation. The typical DJ kind photocatalysts are $RbLnTa_2O_7$ (n = 2) and $KCa_2Nb_3O_{10}$ (n = 3). Associates of the $A_nB_nO_{3n+2}$ and $A_{n+1}B_nO_{3n+3}$ structural sequences with dissimilar layered alignments have also been recognized in some photocatalysts like $Sr_2Ta_2O_7$ and $Sr_5Ta_4O_{15}$ (n = 4). For Aurivillius phases, their frameworks are constructed by one after another fluctuating layers of $[Bi_2O_2]^{2+}$ and virtual perovskite blocks. Bi_2WO_6 and $BiMoO_6$ (n = 1), found as the primary ferroelectric nature for Aurivillius materials, lately have been extensively investigated as visible light photocatalysts.

2.2 Perovskite systems for photocatalysis

A broad array of perovskite photocatalysts have been advanced for organic pollutant degradation in the presence of ultraviolet or visible-light-driven through the last two decades [45]. These typical examples and brief investigational consequences on perovskites are concise giving to their systems, then perovskite materials categorized into six groups. Precisely, ABO_3-type perovskites, AA^IBO_3, A^IABO_3, ABB^IO_3 and $AB(ON)_3$-type perovskites, and $AA^IBB^{II}O_3$-type perovskites are listed in **Table 1**.

2.3 Photocatalytic properties perovskite oxides

$NaTaO_3$ has been a standard perovskite material for a well-organized UV-light photocatalyst for degradation of organic pollutants and production of H_2 and O_2 through water splitting [46–57]. It can be prepared by various methods such as solid-state [46–48, 53, 56], hydrothermal [49, 52, 54, 55], molten salt [57] and sol-gel [50, 51] and with wide bandgap of 4.0 eV. In order to enhance the surface area of $NaTaO_3$ bulk material, many investigators tried to use further synthetic ways to make nanosized particles as an additional study on the $NaTaO_3$ photocatalyst for degradation of organic pollutants. Kondo et al. prepared a colloidal range of $NaTaO_3$ nanoparticles consuming three-dimensional mesoporous carbon as a pattern, which was pretend by the colloidal arrangement of silica nanospheres. After calcining the mesoporous carbon matrix, a colloidal arrangement of $NaTaO_3$ nanoparticles with a range of 20 nm and a surface area of 34 $m^2\ g^{-1}$ was attained. C-doped $NaTaO_3$ material was tested for degradation of NO_x under UV light [36]. Several titanates such as $BaTiO_3$ [58–60], Rh or Fe-doped $BaTiO_3$ [61, 62], $CaTiO_3$ [63, 64] and Cu [65], Rh [66], Ag and La-doped $CaTiO_3$ [67], and $PbTiO_3$ [68, 69] were also described as UV or visible light photocatalysts. Magnetic $BiFeO_3$, recognized as the one of the multi-ferric perovskite materials in magnetoelectric properties, was also examined as a visible light photocatalyst for photodegradation of organic pollutants because of small bandgap energy (2.2 eV) [70–79]. In a previous account, $BiFeO_3$ with a bandgap of around 2.18 eV produced by a citric acid-supported sol-gel technique has revealed its visible-light-driven photocatalytic study by the disintegration of methyl orange dye [70]. The subsequent investigations on $BiFeO_3$ are primarily concentrated on the synthesis of new framework $BiFeO_3$ with various morphologies. For instance, Lin and Nan et al. prepared $BiFeO_3$ unvarying microspheres and microcubes by a using hydrothermal technique as revealed in **Figure 2** [73].

The bandgap energies of $BiFeO_3$ compounds were found to be about 1.82 eV for $BiFeO_3$ microspheres and 2.12–2.27 eV for microcubes. This indicated that the absorption edge was moved toward the longer wavelength that is influenced by the crystal-field strength, particle size, and morphology. The microcube material showed the maximum photocatalytic degradation performance of congo red dye under visible-light irradiation due to the quite low bandgap energy. Further, a simplistic aerosol-spraying method was established for the synthesis of mesoporous $BiFeO_3$ hollow spheres with improved activity for the photodegradation of RhB dye and 4-chlorophenol, because of improved light absorbance ensuing from various light reflections in a hollow chamber and a very high surface area [71]. Moreover, a unusually improved water oxidation property on Au nanoparticle-filled $BiFeO_3$ nanowires under visible-light-driven was described [77]. The Au-$BiFeO_3$ hybrid system was encouraged by the electrostatic contact of negatively charged Au nanoparticles and positively charged $BiFeO_3$ nanowires at pH 6.0 giving to their various isoelectric points. An improved absorbance between 500 and 600 nm was found for Au/$BiFeO_3$ systems because of the characteristic Au surface plasmon band

existing visible light region then which greater influenced in the photodegradation of organic pollutants. Also, the study of photoluminescence supported improvement of the photocatalytic property due to the effective charge transfer from $BiFeO_3$ to Au. Even though Ba, Ca, Mn, and Gd-doped $BiFeO_3$ nanomaterials have exhibited noticeable photocatalytic property for the degradation of dyes [80–84], several nano-based $LaFeO_3$ with various morphologies such as nanoparticles, nanorods, nanotubes, nanosheets, and nanospheres have also been synthesized for visible light photocatalysts for degradation of organic dyes [85–93]. Sodium bismuth titanate ($Bi_{0.5}Na_{0.5}TiO_3$) has been extensively used for ferroelectric and piezoelectric devices. It was also investigated as a UV-light photocatalyst with a bandgap energy of 3.0 eV [94–97]. Hierarchical micro/nanostructured $Bi_{0.5}Na_{0.5}TiO_3$ was produced by in situ self-assembly of $Bi_{0.5}Na_{0.5}TiO_3$ nanocrystals under precise hydrothermal conditions, through the evolution mechanism was examined in aspect means that during which the growth mechanism was studied [95]. It was anticipated that the hierarchical nanostructure was assembled through a method of nucleation and growth and accumulation of nanoparticles and following in situ dissolution-recrystallization of the microsphere type nanoparticles with extended heating period and enhanced temperature or basic settings. The 3D hierarchical $Bi_{0.5}Na_{0.5}TiO_3$ showed very high photocatalytic activity for the decomposition of methyl orange dye because of the adsorption of dye molecules and bigger surface area. The properties of $Bi_{0.5}Na_{0.5}TiO_3$ were also assessed by photocatalytic degradation of nitric oxide in the gas phase [95]. $La_{0.7}Sr_{0.3}MnO_3$, acting as a photocatalyst, was examined for solar light-based photocatalytic decomposition of methyl orange [96–98]. In addition, $La_{0.5}Ca_{0.5}NiO_3$ [99], $La_{0.5}Ca_{0.5}CoO_{3-\delta}$ [100], and $Sr_{1-x}Ba_xSnO_3$ (x = 0–1) [101] nanoparticles were synthesized for revealing improved photocatalytic degradation of dyes. A-site strontium-based perovskites such as $SrTi_{1-x}Fe_xO_{3-\delta}$, $SrTi_{0.1}Fe_{0.9}O_{3-\delta}$, $SrNb_{0.5}Fe_{0.5}O_3$, and $SrCo_{0.5}Fe_{0.5}O_{3-\delta}$ compounds were prepared through solid-state reaction and sol-gel approaches, and were examined for the degradation of organic pollutants under visible light irradiation [102–105]. Also, some other researchers modified A-site with lanthanum-based perovskites such as $LaNi_{1-x}Cu_xO_3$ and $LaFe_{0.5}Ti_{0.5}O_3$ were confirmed as effective visible light photocatalysts for the photodegradation of p-chlorophenol [91, 106, 107]. The other ABB^IO_3 kind photocatalysts with $Ca(TiZr)O_3$ [108], $Ba(ZrSn)O_3$ [109], $Na(BiTa)O_3$ [110], $Na(TiCu)O_3$ [111], $Bi(MgFeTi)O_3$ [112], and $Ag(TaNb)O_3$ [113] have also been studied. Related to AA^IBO_3-type perovskites, the ABB^IO_3 kind system means that BI-site substitution by a different cation is another option for tuning the physicochemical or photocatalytic properties of perovskites materials as photocatalyst, due to typically the B-position cations in ABO_3 mostly regulate the position of the conduction band, moreover to construct the structure of perovskite system with oxygen atoms. The band positions of photocatalyst can be magnificently modified by sensibly coalescing dual or ternary metal cations at the B-position, or changing the ratio of several cations, which has been fine verified by the various materials as mentioned above. More studies on ABB^IO_3 kind of photocatalysts are projected to show their new exhilarating photocatalytic efficiency.

The mesoporous nature of $LaTiO_2N$ of photocatalyst attended due to thermal ammonolysis process of $La_2Ti_2O_7$ precursor from polymer complex obtained from the solid-state reaction. The oxynitride analysis revealed that the pore size and shape, lattice defects and local defects, and oxidation states' local analysis related between morphology and photocatalytic activity were reported by Pokrant et al. [114]. Due to the high capability of accommodating an extensive array of cations and valences at both A- and B-sites, ABO_3-kind perovskite materials are capable materials for fabricating solid-solution photocatalysts. On the other hand, equally the A and B cations can be changed by corresponding cations subsequent in a perovskite with the formula of $(ABO_3)_x(A^IB^IO_3)_{1-x}$. Additional solid solution examples with $CaZrO_3$–$CaTaO_2N$

[115], $SrTiO_3$–$LaTiO_2N$ [116], $La_{0.8}Ba_{0.2}Fe_{0.9}Mn_{0.1}O_{3-x}$ [117], $Na_{1-x}La_xFe_{1-x}Ta_xO_3$ [118], $Na_{0.5}La_{0.5}TiO_3$–$LaCrO_3$ [119], Cu-$(Sr_{1-y}Na_y)$-$(Ti_{1-x}Mo_x)O_3$ [120], $Na_{1-x}La_xTa_{1-x}Cr_xO_3$ [121], $BiFeO_3$–$(Na_{0.5}Bi_{0.5})TiO_3$ [122], and $Sr_{1-x}Bi_xTi_{1-x}Cr_xO_3$ [123] have been used as photocatalysts for splitting of water molecules under visible light.

2.4 Photocatalytic activity of layered perovskite materials

In the general formula of the RP phase, $A_{n-1}A_2^IB_nO_{3n+1}$, A and A^I are alkali, alkaline earth, or rare earth metals, respectively, while B states to transition metals. A and A^I cations are placed in the perovskite layer and boundary with 12-fold cuboctahedral and 9-fold coordination to the anions, respectively, whereas B cations are sited inside the perovskite system with anionic squares, octahedra, and pyramids. The tantalum-based RP phase materials have been examined as photocatalysts for degradation of organic pollutants under UV light irradiation conditions; such materials are $K_2Sr_{1.5}Ta_3O_{10}$ [124], $Li_2CaTa_2O_7$ [125], $H_{1.81}Sr_{0.81}Bi_{0.19}Ta_2O_7$ [126], and N-alkyl chain inserted $H_2CaTa_2O_7$ [127]. A series of various metals and N-doped perovskite materials were synthesized, such as Sn, Cr, Zn, V, Fe, Ni, W, and N-doped $K_2La_2Ti_3O_{10}$, for photocatalysis studies under UV and visible light irradiation [128–133]. Still, only Sn-doping efficiently decreased the bandgap energy of $K_2La_2Ti_3O_{10}$ from 3.6 eV to 2.7 eV. The bandgap energy of N-doped $K_2La_2Ti_3O_{10}$ was measured to be around 3.4 eV. Additional RP phase kind titanates like Sr_2SnO_4 [134], $Sr_3Ti_2O_7$ [135], Cr-doped Sr_2TiO_4 [136], $Sr_4Ti_3O_{10}$ [137], $Na_2Ca_2Nb_4O_{13}$ [138], and Rh- and Ln-doped $Ca_3Ti_2O_7$ [139] have also been examined. Bi_2WO_6 (2.8 eV) shows very high oxygen evolution efficacy than Bi_2MoO_6 (3.0 eV) from aqueous $AgNO_3$ solution under visible-light-driven. Because of the appropriate bandgap energy, comparatively elevated photocatalytic performance, and good constancy, Bi_2MO_6 materials have been thoroughly examined as the Aurivillius phase kind that acts as photocatalysts under visible light. In this connection, hundreds of publications associated to the Bi_2MoO_6 and Bi_2WO_6 act as photocatalysts so far reported. Most of the investigations in the reports are concentrated on the synthesis of various nanostructured Bi_2MoO_6 and Bi_2WO_6 as well as nanofibers, nanosheets, ordered arrays, hollow spheres, hierarchical architectures, inverse opals, and nanoplates, etc., by various synthesis techniques like solvothermal, hydrothermal, electrospinning, molten salt, thermal evaporation deposition, and microwave. All these methods of hydrothermal process have been frequently working for the controlled sizes, shapes, and morphologies of the particles. The photocatalytic properties of these perovskite materials are mostly examined by the photodegradation of organic pollutants. Moreover, the investigations on the simple Bi_2MoO_6 and Bi_2WO_6, doped with various metals and nonmetals such as Zn, Er, Mo, Zr, Gd, W, F, and N, into Bi_2MoO_6 and Bi_2WO_6 was studied for increasing the photocatalytic performance under visible light. Therefore, these Bi_2MO_6-based photocatalysts is not specified here, due to further full deliberations that can be shown in many reviews [140–142].

$ABi_2Nb_2O_9$ where A is Ca, Sr, Ba and Pb is other type of the AL-like layered perovskite material [143–150]. The bandgap energy of $PbBi_2Nb_2O_9$ is 2.88 eV and originally described as an undoped with single-phase layered-type perovskite material used as photocatalyst employed under visible light irradiation [144]. $Bi_5FeTi_3O_{15}$ is also Aurivillius (AL) type multi-layered nanostructured perovskite material with a low bandgap energy (2.1 eV) and also shows photocatalytic activity under visible light [151, 152]. Mostly, these materials were synthesized using the hydrothermal method that has been frequently working for the controlled shapes such as flower-like hierarchical morphology, nanoplate-based, and the complete advance process from nanonet-based to nanoplate-based micro-flowers was shown. The photocatalytic activity of $Bi_5FeTi_3O_{15}$ was studied by the degradation of rhodamine

B and acetaldehyde under visible light [151]. The La substituted $Bi_{5-x}La_xTi_3FeO_{15}$ (x = 1, 2) Al-type layered materials were synthesized through hydrothermal method and these materials were used for photodegradation of rhodamine B under solar-light irradiation [153]. Among all AL-type perovskite materials, only $PbBi_2Nb_2O_9$, Bi_2MO_6 (M = W or Mo), and $Bi_5Ti_3FeO_{15}$ are very high photocatalytic active under visible-light-driven due to low bandgap energy and photostability. Another type of layered perovskite material is Dion-Jacobson phase (DJ), a simple example is $CsBa_2M_3O_{10}$ (M = Ta, Nb) and oxynitride crystals used for degradation of caffeine from wastewater under UVA- and visible-light-driven [154]. Similarly, another DJ phase material such means Dion–Jacobsen (DJ) as $CsM_2Nb_3O_{10}$ (M = Ba and Sr) and also doped with nitrogen used for photocatalysts for degradation of methylene blue [155]. Zhu et al. prepared tantalum-based {111}-layered type of perovskite material such as $Ba_5Ta_4O_{15}$ from hydrothermal method, which has been frequently employed for the controlled shape like hexagonal structure with nanosheets and used as photocatalyst for photodegradation of rhodamine B and gaseous formaldehyde [156]. Pola et al. synthesized a layered-type perovskite material constructed on $A^IA^{II}Ti_2O_6$ (A^I = Na or Ag or Cu and A^{II} = La) structure for the photodegradation of several organic pollutants and industrial wastewater under visible-light-driven [157–162].

Perovskite system	Synthesis process	Light source	Pollutants	References
$NaTaO_3$	HT	UV	CH_3CHO	[163]
La-doped $NaTaO_3$	SG	UV	MB	[164]
La-doped $NaTaO_3$	HT	UV	MB	[165]
Cr-doped $NaTaO_3$	HT	UV	MB	[166]
Eu-doped $NaTaO_3$	SS	UV	MB	[167]
Bi-doped $NaTaO_3$	SS	UV	MB	[168]
N-doped $NaTaO_3$	SS	UV	MB	[169]
C-doped $NaTaO_3$	HT	Visible	NO_x	[36]
N/F co-doped $NaTaO_3$	HT	UV	RhB	[170]
$SrTiO_3$	HT	UV	RhB	[42, 43, 171]
Fe-doped $SrTiO_3$	SG	Visible	RhB	[172]
N-doped $SrTiO_3$	HT	Visible	MB, RhB, MO	[173]
F-doped $SrTiO_3$	BM	Visible	NO	[174]
Ni/La-doped $SrTiO_3$	SG	Visible	MG	[175]
S/C co-doped $SrTiO_3$	SS	Visible	2-Propanol	[176]
N/La-doped $SrTiO_3$	SG	Visible	2-Propanol	[177]
Fe-doped $SrTiO_3$	ST	Visible light	TC	[178]
$SrTiO_3/Fe_2O_3$	HT	Visible	TC	[179]
$BaTiO_3$	SG	UV	Pesticide	[36]
$BaTiO_3$	SG	UV	Aromatics	[58]
$BaTiO_3$	HT	UV	MO	[58]
$KNbO_3$	HT	Visible	RhB	[180]
$KNbO_3$	HT	UV	RhB	[181]
$KNbO_3$	HT	Visible	MB	[182]
$NaNbO_3$	SS	UV	RhB	[183]
$NaNbO_3$	Imp.	UV	2-Propanol	[184]
$NaNbO_3$	SS	UV	MB	[185]

Perovskite system	Synthesis process	Light source	Pollutants	References
N-doped $NaNbO_3$	SS	UV	2-Propanol	[186–188]
Ru-doped $NaNbO_3$	HT	Visible	Phenol	[189]
$AgNbO_3$	SS	UV	MB	[190]
La-doped $AgNbO_3$	SS	Visible	2-Propanol	[191]
$BiFeO_3$	SG	UV-Vis	MO, RhB, 4-CP	[69– 77]
Ba-doped $BiFeO_3$	ES	Visible	CR	[79]
Ca-doped $BiFeO_3$	ES	Visible	CR	[80]
Ba or Mn-doped $BiFeO_3$	ES	Visible	CR	[82]
Ca or Mn-doped $BiFeO_3$	HT	UV-Visible	RhB	[82]
Gd-doped $BiFeO_3$	SG	Visible	RhB	[83]
$LaFeO_3$	Comb.	UV	Methyl phenol	[84]
$LaFeO_3$	SG	Visible	RhB	[85]
$LaFeO_3$	HT	Visible	RhB, MB, chlorophenol	[86, 90, 91, 192]
Ca-doped $LaFeO_3$	SS	Visible	MB	[92]
$LnFeO_3$ (Pr,Y)	SG	Visible	RhB	[193]
$SrFeO_{3-x}$	US	Visible	Phenol	[194]
$SrFeO_3$	SS	Visible	MB	[195]
$BaZrO_3$	SG	UV	MB	[196]
$BaZrO_3$	HT	UV	MO	[197]
$ATiO_3$ (A = Fe, Pb) and $AFeO_3$ (A = Bi, La, Y)	SG	Visible	MB	[198]
$Zn_{0.9}Mg_{0.1}TiO_3$	SG	Visible	MB	[199]
$SrTiO_3$ nanocube-coated CdS microspheres	HT	Visible	Antibiotic pollutants	[200]
Ag/AgCl/$CaTiO_3$	HT	Visible	RhB	[201]
TiO_2-coupled $NiTiO_3$	SS	Visible	MB	[202]
$ZnTiO_3$	HT	UV	MO and PCP	[203]
Mg-doped $BaZrO_3$	SS	UV	MB	[204]
$SrSnO_3$	MW	UV	MO	[205]
$LaCoO_3$	MW	Visible	MO	[206]
$LaCoO_3$	Ads.	UV	MB, MO	[207]
$LaCoO_3$	ES	UV	RhB	[208]
$LaNiO_3$	SG	Visible	MO	[209]
$Bi_{0.5}Na_{0.5}TiO_3$	HT	UV	MO	[93]
$La_{0.7}Sr_{0.3}MnO_3$	SG	Solar light	MO	[97]
$La_{0.5}Ca_{0.5}NiO_3$	SG	UV	RB5	[98]
$La_{0.5}Ca_{0.5}CoO_3$	SG	UV	CR	[99]
$Sr_{1-x}Ba_xSnO_3$	SS	UV	Azo-dye	[100]
$BaCo_{1/2}Nb_{1/2}O_3$	SG	Visible	MB	[210]
$Ba(In_{1/3}Pb_{1/3}M_{1/3})O_3$ (M = Nb and Ta)	SS	Visible	MB, 4-CP	[211]
$A(In_{1/3}Nb_{1/3}B_{1/3})O_3$ (A = Sr, Ba; B = Sn, Pb)	SS	Visible	MB, 4-CP	[212]
$SrTi_{1-x}Fe_xO_{3-\delta}$	SS	Visible	MB	[102]

Perovskite system	Synthesis process	Light source	Pollutants	References
$SrTi_{0.1}Fe_{0.9}O_{3-\delta}$	SG	Solar light	MO	[103]
$SrFe_{0.5}Co_{0.5}O_{3-\delta}$	SG	Solar light	CR	[213]
$LaFe_{0.5}Ti_{0.5}O_3$	SG	UV	Phenol	[90]
$Bi(Mg_{3/8}Fe_{2/8}Ti_{3/8})O_3$	MS	Visible	MO	[110]
$LaTi(ON)_3$	SG	Visible	Acetone	[214]
$(Ag_{0.75}Sr_{0.25})(Nb_{0.75}Ti_{0.25})O_3$	SS	Visible	CH_3CHO	[215]
$La_{0.8}Ba_{0.2}Fe_{0.9}Mn_{0.1}O_{3-x}$	SG	Solar light	MO	[115]
$Cu\text{-}(Sr_{1-y}Na_y)(Ti_{1-x}Mo_x)O_3$	HT	Visible	Propanol	[118]
$BiFeO_3–(Na_{0.5}Bi_{0.5})TiO_3$	SG	Visible	RhB	[120]
$SrBi_2Nb_2O_9$	SG SS	UV	Aniline, RhB	[145, 146]
$ABi_2Nb_2O_9$ (A = Sr, Ba)	SG	UV	MO	[147]
$Bi_5Ti_3FeO_{15}$	HT SS	Visible	RhB, CH_3CHO IPA	[149, 150]
$Bi_{5-x}La_xTi_3FeO_{15}$	SS	Solar light	RhB	[151]
$Bi_3SrTi_2TaO_{12}$ $Bi_2LaSrTi_2TaO_{12}$	SS	UV	RhB	[216]
$Ba_5Ta_4O_{15}$	HT	UV	RhB	[154]
N-doped $Ln_2Ti_2O_7$ (Ln = La, Pr, Nd)	HT	Visible	MO	[217]
$CdS/Ag/Bi_2MoO_6$	SG	Visible	RhB	[218]

SS: solid state; HT: hydrothermal; SG: sol-gel; BM: ball-milling; ES: electronspun; MW: microwave; Comb.: combustion; US: ultrasonic; MS: molten salt; Imp.: impregnation; Ads.: adsorption; ST: solvothermal; RhB: rhodamine B; MO: methyl orange; MB: methylene blue; 4-cp: 4-chlorophenol; MG: malachite green; CR: congo red; NO: nitrogen monoxide; PA: isopropyl alcohol; TC: tetracycline; and PCP: pentachlorophenol.

Table 1.
Perovskite materials used as photocatalysts (ABO_3, AA^IBO_3, AA^IBO_3, ABB^IO_3, $AB(ON)_3$, and $AA^IBB^{II}O_3$) for degradation of pollutants.

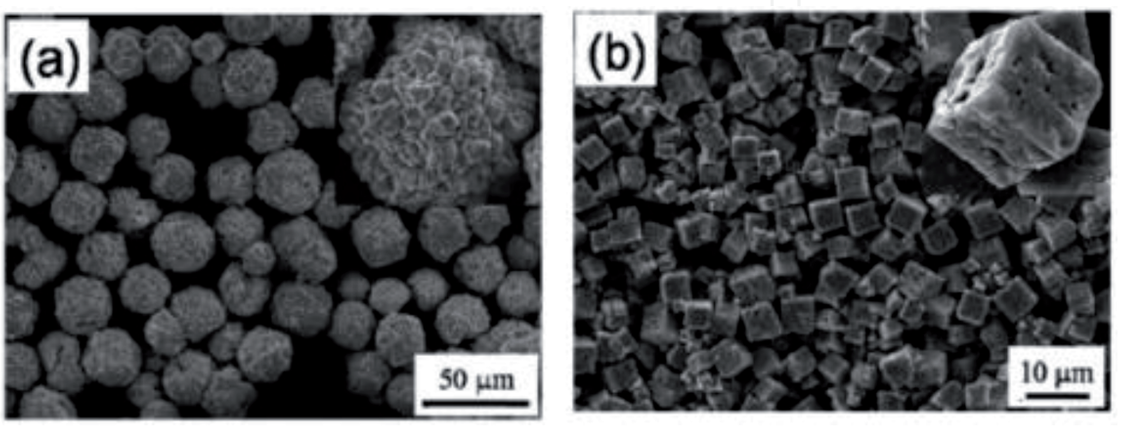

Figure 2.
SEM patterns of $BiFeO_3$: (a) microspheres and (b) microcubes. The intensified pictures are revealed in the upper part inserts. Recopied with consent from Ref. [147]. Copyright © 2010, American Chemical Society.

Acknowledgements

Authors would like to thank DST-FIST schemes and CSIR, New Delhi. One of us (Ramesh Gade) thanks Council of Scientific & Industrial Research (CSIR), New Delhi, for the award of Junior Research Fellowship.

Thanks

I am thankful to Department of Chemistry, University College of Science, Osmania University, for their continuous attention in this study and useful discussions, and to Prof. B. Manohar for her support in working on the chapter.

Author details

Someshwar Pola* and Ramesh Gade
Department of Chemistry, University College of Science, Osmania University, Hyderabad, Telangana, India

*Address all correspondence to: somesh.pola@gmail.com

References

[1] Barbara DA, Jared JS, Tyson AB, William WA. Insights from placing photosynthetic light harvesting into context. Journal of Physical Chemistry Letters. 2014;**5**:2880-2889

[2] von Erika S, Paul SM, James DA, Lori B, Piers F, David F, et al. Chemistry and the linkages between air quality and climate change. Chemical Reviews. 2015;**115**:3856-3897

[3] Rowan JB, Andrew TH. Review of major design and scale-up considerations for solar photocatalytic reactors. Industrial and Engineering Chemistry Research. 2009;**48**:8890-8905

[4] Michael GW, Emily LW, James RM, Shannon WB, Qixi M, Elizabeth AS, et al. Solar water splitting cells. Chemical Reviews. 2010;**110**:6446-6473

[5] Manvendra P, Rahul K, Kamal K, Todd M, Charles UP Jr, Dinesh M. Pharmaceuticals of emerging concern in aquatic systems: Chemistry, occurrence, effects, and removal methods. Chemical Reviews. 2019;**119**:3510-3673

[6] Marta M, Jolanta K, Iseult L, Marianne M, Jan K, Steve B, et al. Changing environments and biomolecule coronas: Consequences and challenges for the design of environmentally acceptable engineered nanoparticles. Green Chemistry. 2018;**20**:4133-4168

[7] Wanjun W, Guiying L, Dehua X, Taicheng A, Huijun Z, Po KW. Photocatalytic nanomaterials for solar-driven bacterial inactivation: recent progress and challenges. Environmental Science: Nano. 2017;**4**:782-799

[8] Wanjun WYY, Taicheng A, Guiying L, Ho YY, Jimmy CY, Po KW. Visible-light-driven photocatalytic inactivation of *E. coli* K-12 by bismuth vanadate nanotubes: bactericidal performance and mechanism. Environmental Science & Technology. 2012;**46**:4599-4606

[9] Nadine C, Stefanie I, Elisabeth S, Marjan V, Karolin K, David D, et al. Inactivation of antibiotic resistant bacteria and resistance genes by ozone: From laboratory experiments to full-scale wastewater treatment. Environmental Science & Technology. 2016;**50**:11862-11871

[10] Yidong Z, Xiangxue W, Ayub K, Pengyi W, Yunhai L, Ahmed A, et al. Environmental remediation and application of nanoscale zero-valent iron and its composites for the removal of heavy metal ions: A review. Environmental Science & Technology. 2016;**50**:7290-7304

[11] Wenya H, Kelong A, Xiaoyan R, Shengyan W, Lehui L. Inorganic layered ion-exchangers for decontamination of toxic metal ions in aquatic systems. Journal of Materials Chemistry A. 2017;**5**:19593-19606

[12] Manolis JM, Mercouri GK. Metal sulfide ion exchangers: Superior sorbents for the capture of toxic and nuclear waste-related metal ions. Chemical Science. 2016;**7**:4804-4824

[13] Chunli K, Kunkun X, Yuhan W, Dongmei H, Ling Z, Fang L, et al. Synthesis of $SrTiO_3$–TiN nanocomposites with enhanced photocatalytic activity under simulated solar irradiation. Industrial and Engineering Chemistry Research. 2018;**57**:11526-11534

[14] Vaidyanathan S, Ryan KR, Eduardo EW. Synthesis and UV–visible-light photoactivity of noble-metal–$SrTiO_3$ composites. Industrial and Engineering Chemistry Research. 2006;**45**:2187-2193

[15] Partha M, Aarthi T, Giridhar M, Srinivasan N. Photocatalytic Degradation of Dyes and Organics with Nanosized $GdCoO_3$. Journal of Physical Chemistry C. 2007;**111**(4):1665-1674

[16] Dipankar S, Sudarshan M, Guru Row TN, Giridhar M. Synthesis, structure, and photocatalytic activity in orthorhombic perovskites $LnVO_3$ and $Ln_{1-x}Ti_xVO_3$ (Ln = Ce, Pr, and Nd). Industrial and Engineering Chemistry Research. 2009;**48**:7489-7497

[17] Barrocas B, Sério S, Rovisco A, Melo Jorge ME. Visible-light photocatalysis in $Ca_{0.6}Ho_{0.4}MnO_3$ films deposited by RF-magnetron sputtering using nanosized powder compacted target. Journal of Physical Chemistry C. 2014;**118**:590-597

[18] Tokeer A, Umar F, Ruby P. Fabrication and photocatalytic applications of perovskite materials with special emphasis on alkali-metal-based niobates and tantalates. Industrial and Engineering Chemistry Research. 2018;**57**:18-41

[19] Senthilkumar P, Arockiya Jency D, Kavinkumar T, Dhayanithi D, Dhanuskodi S, Umadevi M, et al. Built-in electric field assisted photocatalytic dye degradation and photoelectrochemical water splitting of ferroelectric Ce doped $BaTiO_3$ nanoassemblies. ACS Sustainable Chemistry & Engineering. 2019;**7**:12032-12043

[20] Hongbo F, Shicheng Z, Tongguang X, Yongfa Z, Jianmin C. Photocatalytic degradation of RhB by fluorinated Bi_2WO_6 and distributions of the intermediate products. Environmental Science & Technology. 2008;**42**:2085-2091

[21] Sandeep K, Sunita K, Meganathan T, Ashok KG. Achieving enhanced visible-light-driven photocatalysis using type-II $NaNbO_3$/CdS core/shell heterostructures. ACS Applied Materials & Interfaces. 2014;**6**:13221-13233

[22] Yanlong T, Binbin C, Jiangli L, Jie F, Fengna X, Xiaoping D. Hydrothermal synthesis of graphitic carbon nitride–Bi_2WO_6 heterojunctions with enhanced visible light photocatalytic activities. ACS Applied Materials & Interfaces. 2013;**5**:7079-7085

[23] Anindya SP, Gaurangi G, Mohammad Q. Ordered–disordered $BaZrO_{3-\delta}$ hollow nanosphere/carbon dot hybrid nanocomposite: A new visible-light-driven efficient composite photocatalyst for hydrogen production and dye degradation. ACS Omega. 2018;**3**:10980-10991

[24] Joanna HC, Matthew SD, Robert GP, Christopher PI, James RD, John BC, et al. Visible light photo-oxidation of model pollutants using $CaCu_3Ti_4O_{12}$: An experimental and theoretical study of optical properties, electronic structure, and selectivity. Journal of the American Chemical Society. 2011;**133**:1016-1032

[25] Rasel D, Chad DV, Agnes S, Bin C, Ahmad FI, Xianbo L, et al. Recent advances in nanomaterials for water protection and monitoring. Chemical Society Reviews. 2017;**46**:6946-7020

[26] Pena MA, Fierro JLG. Chemical structures and performance of perovskite oxides. Chemical Reviews. 2001;**101**:1981-2018

[27] Anna K, Marcos FG, Gerardo C. Advanced nanoarchitectures for solar photocatalytic applications. Chemical Reviews. 2012;**112**:1555-1614

[28] Wei W, Moses OT, Zongping S. Research progress of perovskite materials in photocatalysis- and photovoltaics-related energy conversion and environmental treatment. Chemical Society Reviews. 2015;**44**:5371-5408

[29] Guan Z, Gang L, Lianzhou W, John TSI. Inorganic perovskite photocatalysts for solar energy utilization. Chemical Society Reviews. 2016;**45**:5951-5984

[30] Xiubing H, Guixia Z, Ge W, John TSI. Synthesis and applications of nanoporous perovskite metal oxides. Chemical Science. 2018;**9**:3623-3637

[31] Beata B, Ewa K, Joanna N, Zhishun W, Maya E, Bunsho O, et al. Preparation of CdS and Bi_2S_3 quantum dots co-decorated perovskite-type $KNbO_3$ ternary heterostructure with improved visible light photocatalytic activity and stability for phenol degradation. Dalton Transactions. 2018;**47**:15232-15245

[32] Hamidreza A, Yuan W, Hongyu S, Mehran R, Hongxing D. Ordered meso- and macroporous perovskite oxide catalysts for emerging applications. Chemical Communications. 2018;**54**:6484-6502

[33] Bin L, Gang L, Lianzhou W. Recent advances in 2D materials for photocatalysis. Nanoscale. 2016;**8**:6904-6920

[34] Chunping X, Prasaanth Ravi A, Cyril A, Rafael L, Samuel M. Nanostructured materials for photocatalysis. Chemical Society Reviews. 2019;**48**:3868-3902

[35] Xiaoyun C, Jun X, Yueshan X, Feng L, Yaping D. Rare earth double perovskites: a fertile soil in the field of perovskite oxides. Inorganic Chemistry Frontiers. 2019;**6**:2226-2238

[36] Xiaoyong W, Shu Y, Qiang D, Tsugio S. Preparation and visible light induced photocatalytic activity of C-$NaTaO_3$ and C-$NaTaO_3$–Cl-TiO_2 composite. Physical Chemistry Chemical Physics. 2013;**15**:20633-20640

[37] Shaodong S, Xiaojing Y, Qing Y, Zhimao Y, Shuhua L. Mesocrystals for photocatalysis: A comprehensive review on synthesis engineering and functional modifications. Nanoscale Advances. 2019;**1**:34-63

[38] Ming Y, Xian LH, Shicheng Y, Zhaosheng L, Tao Y, Zhigang Z. Improved hydrogen evolution activities under visible light irradiation over $NaTaO_3$ codoped with lanthanum and chromium. Materials Chemistry and Physics. 2010;**121**:506-510

[39] Shin S, Yonemura M. Order-disorder transition of $Sr2Fe_2O_5$ from brownmillerite to perovskite structure at an elevated temperature. Materials Research Bulletin. 1978;**13**:1017-1021

[40] Wagner FT, Somorjai GA. Photocatalytic and photoelectro-chemical hydrogen production on strontium titanate single crystals. Journal of the American Chemical Society. 1980;**102**:5494-5502

[41] Guowei L, Graeme RB, Thomas TMP. Vacancies in functional materials for clean energy storage and harvesting: The perfect imperfection. Chemical Society Reviews. 2017;**46**:1693-1706

[42] Xiao W, Gang X, Zhaohui R, Chunxiao X, Ge S, Gaorong H. PVA-assisted hydrothermal synthesis of $SrTiO_3$ nanoparticles with enhanced photocatalytic activity for degradation of RhB. Journal of the American Ceramic Society. 2008;**91**:3795-3799

[43] Xiao W, Gang X, Zhaohui R, Chunxiao X, Wenjian W, Ge S, et al. Single-crystal-like mesoporous $SrTiO_3$ spheres with enhanced photocatalytic performance. Journal of the American Ceramic Society. 2010;**93**:1297-1305

[44] Bo W, Ming-Yu Q, Chuang H, Zi-Rong T, Yi-Jun X. Photocorrosion inhibition of semiconductor-based photocatalysts: Basic principle, current development, and future perspective. ACS Catalysis. 2019;**9**:4642-4687

[45] Natalita MN, Xingdong W, Rachel AC. High-throughput synthesis and screening of titania-based photocatalysts. ACS Combinatorial Science. 2015;**17**:548-569

[46] Hideki K, Akihiko K. Highly efficient decomposition of pure water into H_2 and O_2 over $NaTaO_3$ photocatalysts. Catalysis Letters. 1999;**58**:153-155

[47] Hideki K, Akihiko K. Water splitting into H_2 and O_2 on alkali tantalate photocatalysts $ATaO_3$ (A = Li, Na, and K). Journal of Physical Chemistry B. 2001;**105**(19):4285-4292

[48] Hideki K, Akihiko K. Photocatalytic water splitting into H_2 and O_2 over various tantalate photocatalysts. Catalysis Today. 2003;**78**:561-569

[49] Liu JW, Chen G, Li ZH, Zhang ZG. Hydrothermal synthesis and photocatalytic properties of $ATaO_3$ and $ANbO_3$ (A = Na and K). International Journal of Hydrogen Energy. 2007;**32**:2269-2272

[50] Che-Chia H, Hsisheng T. Influence of structural features on the photocatalytic activity of $NaTaO_3$ powders from different synthesis methods. Applied Catalysis A. 2007;**331**:44-50

[51] Che-Chia H, Chien-Cheng T, Hsisheng T. Structure characterization and tuning of perovskite-like $NaTaO_3$ for applications in photoluminescence and photocatalysis. Journal of the American Ceramic Society. 2009;**92**:460-466

[52] Xia L, Jinling Z. Facile hydrothermal synthesis of sodium tantalate ($NaTaO_3$) nanocubes and high photocatalytic properties. Journal of Physical Chemistry C. 2009;**113**:19411-19418

[53] Fu X, Wang X, Leung DYC, Xue W, Ding Z, Huang H, et al. Photocatalytic reforming of glucose over La doped alkali tantalate photocatalysts for H_2 production. Catalysis Communications. 2010;**12**:184-187

[54] Yokoi T, Sakuma J, Maeda K, Domen K, Tatsumi T, Kondo JN. Preparation of a colloidal array of $NaTaO_3$ nanoparticles via a confined space synthesis route and its photocatalytic application. Physical Chemistry Chemical Physics. 2011;**13**:2563-2570

[55] Shi J, Liu G, Wang N, Li C. Microwave-assisted hydrothermal synthesis of perovskite $NaTaO_3$ nanocrystals and their photocatalytic properties. Journal of Materials Chemistry. 2012;**22**:18808-18813

[56] Meyer T, Priebe JB, Silva RO, Peppel T, Junge H, Beller M, et al. Advanced charge utilization from $NaTaO_3$ photocatalysts by multilayer reduced graphene oxide. Chemistry of Materials. 2014;**26**:4705-4711

[57] Li Y, Gou H, Lu J, Wang C. A two-step synthesis of $NaTaO_3$ microspheres for photocatalytic water splitting. International Journal of Hydrogen Energy. 2014;**39**:13481-13485

[58] Gomathi Devi L, Krishnamurthy G. TiO_2/$BaTiO_3$-assisted photocatalytic mineralization of diclofop-methyl on UV-light irradiation in the presence of oxidizing agents. Journal of Hazardous Materials. 2009;**162**:899-905

[59] Gomathi Devi L, Krishnamurthy G. TiO_2- and $BaTiO_3$-assisted photocatalytic degradation of selected chloroorganic compounds in aqueous medium: Correlation of reactivity/orientation effects of substituent groups of the pollutant molecule on the degradation rate. The Journal of Physical Chemistry. A. 2011;**115**:460-469

[60] Liu J, Sun Y, Li Z. Ag loaded flower-like $BaTiO_3$ nanotube arrays: Fabrication

and enhanced photocatalytic property. CrystEngComm. 2012;**14**:1473-1478

[61] Maeda K. Rhodium-doped barium titanate perovskite as a stable p-type semiconductor photocatalyst for hydrogen evolution under visible light. ACS Applied Materials & Interfaces. 2014;**6**:2167-2173

[62] Upadhyay S, Shrivastava J, Solanki A, Choudhary S, Sharma V, Kumar P, et al. Enhanced photoelectrochemical response of $BaTiO_3$ with Fe doping: Experiments and first-principles analysis. Journal of Physical Chemistry C. 2011;**115**:24373-24380

[63] Mizoguchi H, Ueda K, Orita M, Moon S-C, Kajihara K, Hirano M, et al. Decomposition of water by a $CaTiO_3$ photocatalyst under UV light irradiation. Materials Research Bulletin. 2002;**37**:2401-2406

[64] Shimura K, Yoshida H. Hydrogen production from water and methane over Pt-loaded calcium titanate photocatalyst. Energy & Environmental Science. 2010;**3**:615-617

[65] Zhang H, Chen G, Li Y, Teng Y. Electronic structure and photocatalytic properties of copper-doped $CaTiO_3$. International Journal of Hydrogen Energy. 2010;**35**:2713-2716

[66] Nishimoto S, Matsuda M, Miyake M. Photocatalytic activities of Rh-doped $CaTiO_3$ under visible light irradiation. Chemistry Letters. 2006;**35**:308-309

[67] Zhang H, Chen G, He X, Xu J. Electronic structure and photocatalytic properties of Ag–La codoped $CaTiO_3$. Journal of Alloys and Compounds. 2012;**516**:91-95

[68] Arney D, Watkins T, Maggard PA. Effects of particle surface areas and microstructures on photocatalytic H_2 and O_2 production over $PbTiO_3$. Journal of the American Ceramic Society. 2011;**94**:1483-1489

[69] Zhen C, Yu JC, Liu G, Cheng H-M. Selective deposition of redox co-catalyst(s) to improve the photocatalytic activity of single-domain ferroelectric $PbTiO_3$ nanoplates. Chemical Communications. 2014;**50**:10416-10419

[70] Gao F, Chen X, Yin K, Dong S, Ren Z, Yuan F, et al. Visible-Light photocatalytic properties of weak magnetic $BiFeO_3$ nanoparticles. Advanced Materials. 2007;**19**:2889-2892

[71] Huo Y, Miao M, Zhang Y, Zhu J, Li H. Aerosol-spraying preparation of a mesoporous hollow spherical $BiFeO_3$ visible photocatalyst with enhanced activity and durability. Chemical Communications. 2011;**47**:2089-2091

[72] Cho CM, Noh JH, Cho I-S, An J-S, Hong KS. Low-temperature hydrothermal synthesis of pure $BiFeO_3$ nanopowders using triethanolamine and their applications as visible-light photocatalysts. Journal of the American Ceramic Society. 2008;**91**:3753-3755

[73] Li S, Lin Y-H, Zhang B-P, Wang Y, Nan C-W. Controlled fabrication of $BiFeO_3$ uniform microcrystals and their magnetic and photocatalytic behaviors. Journal of Physical Chemistry C. 2010;**114**:2903-2908

[74] Xu X, Lin Y-H, Li P, Shu L, Nan C-W. Synthesis and photocatalytic behaviors of high surface area $BiFeO_3$ thin films. Journal of the American Ceramic Society. 2011;**94**:2296-2299

[75] Ji W, Yao K, Lim Y-F, Liang YC, Suwardi A. Large modulation of perpendicular magnetic anisotropy in a $BiFeO_3/Al_2O_3/Pt/Co/Pt$ multiferroic heterostructure via spontaneous polarizations. Applied Physics Letters. 2013;**103**:062901

[76] Chen XY, Yu T, Gao F, Zhang HT, Liu LF, Wang YM, et al. Application of weak ferromagnetic $BiFeO_3$ films as the photoelectrode material under visible-light irradiation. Applied Physics Letters. 2007;**91**:022114

[77] Li S, Zhang J, Kibria MG, Mi Z, Chaker M, Ma D, et al. Remarkably enhanced photocatalytic activity of laser ablated Au nanoparticle decorated $BiFeO_3$ nanowires under visible-light. Chemical Communications. 2013;**49**:5856-5858

[78] Huo Y, Jin Y, Zhang Y. Citric acid assisted solvothermal synthesis of $BiFeO_3$ microspheres with high visible-light photocatalytic activity. Journal of Molecular Catalysis A: Chemical. 2010;**331**:15-20

[79] Schultz AM, Zhang Y, Salvador PA, Rohrer GS. Effect of crystal and domain orientation on the visible-light photochemical reduction of Ag on $BiFeO_3$. ACS Applied Materials & Interfaces. 2011;**3**:1562-1567

[80] Feng YN, Wang HC, Shen Y, Lin YH, Nan CW. Magnetic and photocatalytic behaviors of Ba-doped $BiFeO_3$ nanofibers. International Journal of Applied Ceramic Technology. 2014;**11**:676-680

[81] Feng YN, Wang HC, Luo YD, Shen Y, Lin YH. Ferromagnetic and photocatalytic behaviors observed in Ca-doped $BiFeO_3$ nanofibres. Journal of Applied Physics. 2013;**113**:146101

[82] Wang HC, Lin YH, Feng YN, Shen Y. Photocatalytic behaviors observed in Ba and Mn doped $BiFeO_3$ nanofibers. Journal of Electroceramics. 2013;**31**:271

[83] Pei YL, Zhang C. Effect of ion doping in different sites on the morphology and photocatalytic activity of $BiFeO_3$ microcrystals. Journal of Alloys and Compounds. 2013;**570**:57-60

[84] Guo R, Fang L, Dong W, Zheng F, Shen M. Enhanced photocatalytic activity and ferromagnetism in Gd doped $BiFeO_3$ nanoparticles. Journal of Physical Chemistry C. 2010;**114**:21390-21396

[85] Deganello F, Tummino ML, Calabrese C, Testa ML, Avetta P, Fabbi D, et al. A new, sustainable $LaFeO_3$ material prepared from biowaste-sourced soluble substances. New Journal of Chemistry. 2015;**39**:877-885

[86] Li L, Wang X, Zhang Y. Enhanced visible light-responsive photocatalytic activity of $LnFeO_3$ (Ln = La, Sm) nanoparticles by synergistic catalysis. Materials Research Bulletin. 2014;**50**:18-22

[87] Thirumalairajan S, Girija K, Mastelaro VR, Ponpandian N. Photocatalytic degradation of organic dyes under visible light irradiation by floral-like $LaFeO_3$ nanostructures comprised of nanosheet petals. New Journal of Chemistry. 2014;**38**:5480-5490

[88] Parida KM, Reddy KH, Martha S, Das DP, Biswal N. Fabrication of nanocrystalline $LaFeO_3$: An efficient sol–gel auto-combustion assisted visible light responsive photocatalyst for water decomposition. International Journal of Hydrogen Energy. 2010;**35**:12161-12168

[89] Tijare SN, Joshi MV, Padole PS, Mangrulkar PA, Rayalu SS, Labhsetwar NK. Photocatalytic hydrogen generation through water splitting on nano-crystalline $LaFeO_3$ perovskite. International Journal of Hydrogen Energy. 2012;**37**:10451-10456

[90] Thirumalairajan S, Girija K, Ganesh I, Mangalaraj D, Viswanathan C, Balamurugan A. Controlled synthesis of perovskite $LaFeO_3$ microsphere composed of nanoparticles via self-assembly process and their associated photocatalytic activity. Chemical Engineering Journal. 2012;**209**:420-428

[91] Hu R, Li C, Wang X, Sun Y, Jia H, Su H, et al. Photocatalytic activities of $LaFeO_3$ and La_2FeTiO_6 in p-chlorophenol degradation under visible light. Catalysis Communications. 2012;**29**:35-39

[92] Thirumalairajan S, Girija K, Hebalkar NY, Mangalaraj D, Viswanathan C, Ponpandian N. Shape evolution of perovskite $LaFeO_3$ nanostructures: A systematic investigation of growth mechanism, properties and morphology dependent photocatalytic activities. RSC Advances. 2013;**3**:7549-7561

[93] Li FT, Liu Y, Liu RH, Sun ZM, Zhao DS, Kou CG. Preparation of Ca-doped $LaFeO_3$ nanopowders in a reverse microemulsion and their visible light photocatalytic activity. Materials Letters. 2010;**64**:223-225

[94] Invalid reference

[95] Li J, Wang G, Wang H, Tang C, Wang Y, Liang C, et al. In situ self-assembly synthesis and photocatalytic performance of hierarchical $Bi0.5Na0.5TiO_3$ micro/nanostructures. Journal of Materials Chemistry. 2009;**19**:2253-2258

[96] Wang L, Wang W. Photocatalytic hydrogen production from aqueous solutions over novel $Bi0.5Na0.5TiO_3$ microspheres. International Journal of Hydrogen Energy. 2012;**37**:3041-3047

[97] Ai Z, Lu G, Lee S. Efficient photocatalytic removal of nitric oxide with hydrothermal synthesized $Na0.5Bi0.5TiO_3$ nanotubes. Journal of Alloys and Compounds. 2014;**613**:260-266

[98] Hu CC, Lee YL, Teng H. Efficient water splitting over $Na_{1-x}K_xTaO_3$ photocatalysts with cubic perovskite structure. Journal of Materials Chemistry. 2011;**21**:3824-3830

[99] Ghiasi M, Malekzadeh MA. Solar photocatalytic degradation of methyl orange over $La_{0.7}Sr_{0.3}MnO_3$ nano-perovskite. Separation and Purification Technology. 2014;**134**:12-19

[100] Yazdanbakhsh M, Tavakkoli H, Hosseini SM. Characterization and evaluation catalytic efficiency of $La_{0.5}Ca_{0.5}NiO_3$ nanopowders in removal of reactive blue 5 from aqueous solution. Desalination. 2011;**281**:388-395

[101] Tavakkoli H, Beiknejad D, Tabari T. Fabrication of perovskite-type oxide $La_{0.5}Ca_{0.5}CoO_{3-\delta}$ nanoparticles and its dye removal performance. Desalination and Water Treatment. 2014;**52**:7377-7388

[102] Sales HB, Bouquet V, Deputier S, Ollivier S, Gouttefangeas F, Guilloux-Viry G, et al. $Sr_{1-x}Ba_xSnO_3$ system applied in the photocatalytic discoloration of an azo-dye. Solid State Sciences. 2014;**28**:67-73

[103] Bae SW, Borse PH, Lee JS. Dopant dependent band gap tailoring of hydrothermally prepared cubic $SrTi_xM_{1-x}O_3$ (M = Ru, Rh, Ir, Pt, Pd) nanoparticles as visible light photocatalysts. Applied Physics Letters. 2008;**92**:104107

[104] Ghaffari M, Huang H, Tan PY, Tan OK. Synthesis and visible light photocatalytic properties of $SrTi_{(1-x)}Fe_xO_{(3-\delta)}$ powder for indoor decontamination. Powder Technology. 2012;**225**:221-226

[105] Chen HX, Wei ZX, Wang Y, Zeng WW, Xiao CM. Preparation of $SrTi_{0.1}Fe_{0.9}O_{3-\delta}$ and its photocatalysis activity for degradation of methyl orange in water. Materials Chemistry and Physics. 2011;**130**:1387-1393

[106] Jeong ED, Yu SM, Yoon JY, Bae JS, Cho CR, Lim KT, et al. Efficient visible light photocatalysis in cubic Sr_2FeNbO_6. Journal of Ceramic Processing Research. 2012;**13**:305-309

[107] Li J, Jia L, Fang W, Zeng J. Enhancement of activity of $LaNi_{0.7}Cu_{0.3}O_3$ for photocatalytic water splitting by reduction treatment at moderate temperature. International Journal of Hydrogen Energy. 2010;**35**:5270-5275

[108] Li J, Zeng J, Jia L, Fang W. Investigations on the effect of Cu^{2+}/Cu^{1+} redox couples and oxygen vacancies on photocatalytic activity of treated $LaNi_{1-x}Cu_xO_3$ (x = 0.1, 0.4, 0.5). International Journal of Hydrogen Energy. 2010;**35**:12733-12740

[109] Li H, Liang Q, Gao LZ, Tang SH, Cheng ZY, Zhang BL, et al. Catalytic production of carbon nanotubes by decomposition of CH_4 over the pre-reduced catalysts $LaNiO_3$, $La_4Ni_3O_{10}$, $La_3Ni_2O_7$ and La_2NiO_4. Catalysis Letters. 2001;**74**:185-188

[110] Yuan Y, Zhao Z, Zheng J, Yang M, Qiu L, Li Z, et al. Polymerizable complex synthesis of $BaZr_{1-x}SnxO_3$ photocatalysts: Role of Sn^{4+} in the band structure and their photocatalytic water splitting activities. Journal of Materials Chemistry. 2010;**20**:6772-6779

[111] Kang HW, Lim SN, Park SB. Photocatalytic H_2 evolution under visible light from aqueous methanol solution on $NaBi_xTa_{1-x}O_3$ prepared by spray pyrolysis. International Journal of Hydrogen Energy. 2012;**37**:4026-4035

[112] Xu L, Li C, Shi W, Guan J, Sun Z. Visible light-response $NaTa_{1-x}Cu_xO_3$ photocatalysts for hydrogen production from methanol aqueous solution. Journal of Molecular Catalysis A: Chemical. 2012;**360**:42-47

[113] Zhang W, Chen J, An X, Wang Q, Fan L, Wang F, et al. Rapid synthesis, structure and photocatalysis of pure bismuth A-site perovskite of $Bi(Mg_{3/8}Fe_{2/8}Ti_{3/8})O_3$. Dalton Transactions. 2014;**43**:9255-9259

[114] Ni L, Tanabe M, Irie H. A visible-light-induced overall water-splitting photocatalyst: Conduction-band-controlled silver tantalite. Chemical Communications. 2013;**49**:10094-10096

[115] Simone P, Marie CC, Stephan I, Alexandra EM, Rolf E. Mesoporosity in photocatalytically active oxynitride single crystals. Journal of Physical Chemistry C. 2014;**118**(36):20940-20947

[116] Wu P, Shi J, Zhou Z, Tang W, Guo L. $CaTaO_2N$–$CaZrO_3$ solid solution: Band-structure engineering and visible-light-driven photocatalytic hydrogen production. International Journal of Hydrogen Energy. 2012;**37**:13704-13710

[117] Luo W, Li Z, Jiang X, Yu T, Liu L, Chen X, et al. Correlation between the band positions of $(SrTiO_3)_{1-x}{\cdot}(LaTiO_2N)_x$ solid solutions and photocatalytic properties under visible light irradiation. Physical Chemistry Chemical Physics. 2008;**10**:6717-6723

[118] Wei ZX, Xiao CM, Zeng WW, Liu JP. Magnetic properties and photocatalytic activity of $La_{0.8}Ba_{0.2}Fe_{0.9}Mn_{0.1}O_{3-\delta}$ and $LaFe_{0.9}Mn_{0.1}O_{3-\delta}$. Journal of Molecular Catalysis A: Chemical. 2013;**370**:35-43

[119] Kanhere P, Nisar P, Tang Y, Pathak B, Ahuja R, Zheng J, et al. Electronic structure, optical properties, and photocatalytic activities of $LaFeO_3$–$NaTaO_3$ solid solution. Journal of Physical Chemistry C. 2012;**116**:22767-22773

[120] Shi J, Ye J, Zhou Z, Li M, Guo L. Hydrothermal synthesis of $Na_{0.5}La_{0.5}TiO_3$–$LaCrO_3$ solid-solution single-crystal nanocubes for visible-light-driven photocatalytic H_2 evolution. Chemistry—A European Journal. 2011;**17**:7858-7867

[121] Qiu X, Miyauchi M, Yu H, Irie H, Hashimoto K. Visible-light-driven

Cu(II)-$(Sr_{1-y}Na_y)(Ti_{1-x}Mo_x)O_3$ photocatalysts based on conduction band control and surface ion modification. Journal of the American Chemical Society. 2010;**132**:15259-15267

[122] Yi ZG, Ye JH. Band gap tuning of $Na_{1-x}La_xTa_{1-x}Cr_xO_3$ for H_2 generation from water under visible light irradiation. Journal of Applied Physics. 2009;**106**:074910

[123] Liu H, Guo Y, Guo B, Dong W, Zhang D. $BiFeO_3$–$(Na_{0.5}Bi_{0.5})TiO_3$ butterfly wing scales: Synthesis, visible-light photocatalytic and magnetic properties. Journal of the European Ceramic Society. 2012;**32**:4335-4340

[124] Lv M, Xie Y, Wang Y, Sun X, Wu F, Chen H, et al. Bismuth and chromium co-doped strontium titanates and their photocatalytic properties under visible light irradiation. Physical Chemistry Chemical Physics. 2015;**17**:26320-26329

[125] Yao W, Ye J. Photocatalytic properties of a new photocatalyst $K_2Sr_{1.5}Ta_3O_{10}$. Chemical Physics Letters. 2007;**435**:96-99

[126] Liang Z, Tang K, Shao Q, Li G, Zeng S, Zheng H. Synthesis, crystal structure, and photocatalytic activity of a new two-layer Ruddlesden–Popper phase, $Li_2CaTa_2O_7$. Journal of Solid State Chemistry. 2008;**181**:964-970

[127] Li Y, Chen G, Zhou C, Li Z. Photocatalytic water splitting over a protonated layered perovskite tantalate $H_{1.81}Sr_{0.81}Bi_{0.19}Ta_2O_7$. Catalysis Letters. 2008;**123**:80-83

[128] Wang Y, Wang C, Wang L, Hao Q, Zhu X, Chen X, et al. Preparation of interlayer surface tailored protonated double-layered perovskite $H_2CaTa_2O_7$ with n-alcohols, and their photocatalytic activity. RSC Advances. 2014;**4**:4047-4054

[129] Kumar V, Uma GS. Investigation of cation (Sn^{2+}) and anion (N^{3-}) substitution in favor of visible light photocatalytic activity in the layered perovskite $K_2La_2Ti_3O_{10}$. Journal of Hazardous Materials. 2011;**189**:502-508

[130] Thaminimulla CTK, Takata T, Hara M, Knodo JN, Domen K. Effect of chromium addition for photocatalytic overall water splitting on Ni–$K_2La_2Ti_3O_{10}$. Journal of Catalysis. 2000;**196**:362-365

[131] Yang YH, Chen QY, Yin ZL, Li J. Study on the photocatalytic activity of $K_2La_2Ti_3O_{10}$ doped with zinc(Zn). Applied Surface Science. 2009;**255**:8419-8424

[132] Yang Y, Chen Q, Yin Z, Li J. Study on the photocatalytic activity of $K_2La_2Ti_3O_{10}$ doped with vanadium (V). Journal of Alloys and Compounds. 2009;**488**:364

[133] Huang Y, Wei Y, Cheng S, Fan L, Li Y, Lin J, et al. Photocatalytic property of nitrogen-doped layered perovskite $K_2La_2Ti3O10$. Solar Energy Materials and Solar Cells. 2010;**94**:761-766

[134] Wang B, Li C, Hirabayashi D, Suzuki K. Hydrogen evolution by photocatalytic decomposition of water under ultraviolet–visible irradiation over $K_2La_2Ti_{3-x}M_xO_{10+\delta}$ perovskite. International Journal of Hydrogen Energy. 2010;**35**:3306-3312

[135] Sato J, Saito N, Nishiyama H, Inoue Y. New photocatalyst group for water decomposition of RuO_2-loaded p-block metal (In, Sn, and Sb) oxides with d10 Configuration. The Journal of Physical Chemistry. B. 2001;**105**:6061-6063

[136] Jeong H, Kim T, Kim D, Kim K. Hydrogen production by the photocatalytic overall water splitting on $NiO/Sr_3Ti_2O_7$: Effect of preparation method. International Journal of Hydrogen Energy. 2006;**31**:1142-1146

[137] Sun X, Xie Y, Wu F, Chen H, Lv M, Ni S, et al. Photocatalytic hydrogen production over chromium doped layered perovskite Sr_2TiO_4. Inorganic Chemistry. 2015;**54**:7445-7453

[138] Ko YG, Lee WY. Effects of nickel-loading method on the water-splitting activity of a layered $NiO_x/Sr_4Ti_3O_{10}$ photocatalyst. Catalysis Letters. 2002;**83**:157-160

[139] Arney D, Fuoco L, Boltersdorf J, Maggard PA. Flux synthesis of $Na_2Ca_2Nb_4O_{13}$: The influence of particle shapes, surface features, and surface areas on photocatalytic hydrogen production. Journal of the American Ceramic Society. 2012;**96**:1158-1162

[140] Nishimoto S, Okazaki Y, Matsuda M, Miyake M. Photocatalytic H_2 evolution by layered perovskite $Ca_3Ti_2O_7$ codoped with Rh and Ln (Ln = La, Pr, Nd, Eu, Gd, Yb, and Y) under visible light irradiation. Journal of the Ceramic Society of Japan. 2009;**117**:1175-1179

[141] Zhang L, Wang H, Chen Z, Wong PK, Liu J. Bi_2WO_6 micro/nano-structures: Synthesis, modifications and visible-light-driven photocatalytic applications. Applied Catalysis B. 2011;**106**:1-13

[142] Zhang L, Zhu Y. A review of controllable synthesis and enhancement of performances of bismuth tungstate visible-light-driven photocatalysts. Catalysis Science & Technology. 2012;**2**:694-706

[143] Zhang N, Ciriminna R, Ragliaro M, Xu YJ. Nanochemistry-derived Bi_2WO_6 nanostructures: towards production of sustainable chemicals and fuels induced by visible light. Chemical Society Reviews. 2014;**43**:5276-5287

[144] Fu H, Pan C, Yao W, Zhu Y. Visible-light-induced degradation of rhodamine B by nanosized Bi_2WO_6. The Journal of Physical Chemistry. B. 2005;**109**:22432-22439

[145] Kim HG, Hwang DW, Lee JS. An undoped, single-phase oxide photocatalyst working under visible light. Journal of the American Chemical Society. 2004;**126**:8912-8913

[146] Kim HG, Becker OS, Jang JS, Ji SM, Borse PH, Lee JS. A generic method of visible light sensitization for perovskite-related layered oxides: Substitution effect of lead. Journal of Solid State Chemistry. 2006;**179**:1214-1218

[147] Kim HG, Borse PH, Jang JS, Jeong ED, Lee JS. Enhanced photochemical properties of electron rich W-doped $PbBi_2Nb_2O_9$ layered perovskite material under visible-light irradiation. Materials Letters. 2008;**62**:1427-1430

[148] Wu W, Liang S, Chen Y, Shen L, Zheng H, Wu L. High efficient photocatalytic reduction of 4-nitroaniline to p-phenylenediamine over microcrystalline $SrBi_2Nb_2O_9$. Catalysis Communications. 2012;**17**:39-42

[149] Kim JH, Hwang KT, Kim US, Kang YM. Photocatalytic characteristics of immobilized $SrBi_2Nb_2O_9$ film for degradation of organic pollutants. Ceramics International. 2012;**38**:3901-3906

[150] Wu W, Liang S, Wang X, Bi J, Liu P, Wu L. Synthesis, structures and photocatalytic activities of microcrystalline $ABi_2Nb_2O_9$ (A = Sr, Ba) powders. Journal of Solid State Chemistry. 2011;**184**:81-88

[151] Li Y, Chen G, Zhang H, Lv G. Band structure and photocatalytic activities for H_2 production of $ABi_2Nb_2O_9$ (A = Ca, Sr, Ba). International Journal of Hydrogen Energy. 2010;**35**:2652-2656

[152] Sun S, Wang W, Xu H, Zhou L, Shang M, Zhang L. $Bi_5FeTi_3O_{15}$

hierarchical microflowers: Hydrothermal synthesis, growth mechanism, and associated visible-light-driven photocatalysis. Journal of Physical Chemistry C. 2008;**112**:17835-17843

[153] Jang JS, Yoon SS, Borse PH, Lim KT, Hong TE, Jeong ED, et al. Synthesis and characterization of aurivilius phase $Bi_5Ti_3FeO_{15}$layered perovskite for Visible light photocatalysis. Journal of the Ceramic Society of Japan. 2009;**117**:1268-1272

[154] Naresh G, Mandal TK. Excellent sun-light-driven photocatalytic activity by aurivillius layered perovskites, $Bi_{5-x}La_xTi_3FeO_{15}$ (x = 1, 2). ACS Applied Materials & Interfaces. 2014;**6**:21000-21010

[155] Bożena C, Mirabbos H. UVA- and visible-light-driven photocatalytic activity of three-layer perovskite Dion-Jacobson phase $CsBa_2M_3O_{10}$ (M = Ta, Nb) and oxynitride crystals in the removal of caffeine from model wastewater. Journal of Photochemistry and Photobiology A: Chemistry. 2016;**324**:70-80

[156] Reddy JR, Kurra S, Guje R, Palla S, Veldurthi NK, Ravi G, et al. Photocatalytic degradation of methylene blue on nitrogen doped layered perovskites, $CsM_2Nb_3O_{10}$ (M = Ba and Sr). Ceramics International. 2015;**41**:2869-2875

[157] Xu TG, Zhang C, Shao X, Wu K, Zhu YF. Monomolecular-layer $Ba_5Ta_4O_{15}$ nanosheets: Synthesis and investigation of photocatalytic properties. Advanced Functional Materials. 2006;**16**:1599-1607

[158] Ramesh G, Jakeer A, Kalyana LY, Seid YA, Tao YT, Someshwar P. Photodegradation of organic dyes and industrial wastewater in the presence of layer-type perovskite materials under visible light irradiation. Journal of Environmental Chemical Engineering. 2018;**6**:4504-4513

[159] Friedmann D, Mendice C, Bahnemann D. TiO_2 for water treatment: Parameters affecting the kinetics and mechanisms of photocatalysis. Applied Catalysis B: Environmental. 2010;**99**:398-406

[160] Rizzo L, Meric S, Kassino D, Guida M, Russo F, Belgiorno V. Degradation of diclofenac by TiO_2 photocatalysis: UV absorbance kinetics and process evaluation through a set of toxicity bioassays. Water Research. 2009;**43**:979-988

[161] Konstantinou T, Albanis A. TiO_2-assisted photocatalytic degradation of azo dyes in aqueous solution: Kinetic and mechanistic investigations. A review. Applied Catalysis B: Environmental. 2004;**49**:1-14

[162] Kim SH, Ngo HH, Shon HK, Vigneswaran S. Adsorption and photocatalysis kinetics of herbicide onto titanium oxide and powdered activated carbon. Separation and Purification Technology. 2008;**58**:335-342

[163] Liu JW, Chen G, Li ZH, Zhang ZG. Electronic structure and visible light photocatalysis water splitting property of chromium-doped $SrTiO_3$. Journal of Solid State Chemistry. 2006;**179**:3704-3708

[164] Torres-Martínez LM, Cruz-López A, Juárez-Ramírez I, Elena Meza-de la Rosa M. Methylene blue degradation by $NaTaO_3$ sol–gel doped with Sm and La. Journal of Hazardous Materials. 2009;**165**:774-779

[165] Li X, Zang J. Hydrothermal synthesis and characterization of lanthanum-doped $NaTaO_3$ with high photocatalytic activity. Catalysis Communications. 2011;**12**:1380-1383

[166] Yiguo S, Wang S, Meng Y, Wang HHX. Dual substitutions of

single dopant Cr^{3+} in perovskite $NaTaO_3$: synthesis, structure, and photocatalytic performance. RSC Advances. 2012;**2**:12932-12939

[167] Wang B, Kanhere PD, Chen Z, Nisar J, Biswarup PA. Anion-doped $natao_3$ for visible light photocatalysis. Journal of Physical Chemistry C. 2014;**118**:10728-10739

[168] Kanhere PD, Zheng J, Chen Z. Site specific optical and photocatalytic properties of Bi-doped $NaTaO_3$. Journal of Physical Chemistry C. 2011;**115**:11846-11853

[169] Liu D-R, Wei C-D, Xue B, Zhang X-G, Jiang Y-S. Synthesis and photocatalytic activity of N-doped $NaTaO_3$ compounds calcined at low temperature. Journal of Hazardous Materials. 2010;**182**:50-54

[170] Zhang J, Jiang Y, Gao W, Hao H. Synthesis and visible photocatalytic activity of new photocatalyst MBI_2O_4 (M = Cu,Zn). Journal of Materials Science: Materials in Electronics. 2014;**25**:3807-3815

[171] Da Silva LF, Avansi W, Andres J, Ribeiro C. Long-range and short-range structures of cube-like shape $SrTiO_3$ powders: Microwave-assisted hydrothermal synthesis and photocatalytic activity. Physical Chemistry Chemical Physics. 2013;**15**:12386-12393

[172] Xie T-H, Sun X, Lin J. Enhanced photocatalytic degradation of RhB driven by visible light-induced MMCT of Ti(IV)-O-Fe(II)formed in Fe-doped $SrTiO_3$. Journal of Physical Chemistry C. 2008;**112**:9753-9759

[173] Zou F, Zheng J, Qin X, Zhao Y, Jiang L, Zhi J, et al. Chemical Communications. 2012;**48**:8514-8516

[174] Wang J, Yin S, Zhang Q, Saito F, Sato T. Mechanochemical synthesis of $SrTiO_{3-x}F_x$ with high visible light photocatalytic activities for nitrogen monoxide destruction. Journal of Materials Chemistry. 2003;**13**:2348-2352

[175] Jia A, Liang X, Su Z, Zhu T, Liu S. Synthesis and effect of calcinations temperature on the physical-chemical properties and photocatalytic activities of Ni, La coded $SrTiO_3$. Journal of Hazardous Materials. 2010;**178**:233-242

[176] Ohno T, Tsubota T, Nakamura Y, Sayama K. Preparation of S, C cation-codoped $SrTiO_3$ and its photocatalytic activity under visible light. Applied Catalysis A. 2005;**288**:74-79

[177] Miyauchi M, Takashio M, Tobimastu H. Photocatalytic activity of $SrTiO_3$ codoped with nitrogen and lanthanum under visible light illumination. Langmuir. 2004;**20**:232-236

[178] Li P, Liu C, Wu G, Yang H, Lin S, Ren A, et al. Solvothermal synthesis and visible light-driven photocatalytic degradation for tetracycline of Fe-doped $SrTiO_3$. RSC Advances. 2014;**4**:47615-47624

[179] Liu C, Wu G, Chen J, Hang K, Shi W. Fabrication of a visible-light-driven photocatalyst and degradation of tetracycline based on the photoinduced interfacial charge transfer of $SrTiO_3$/Fe_2O_3 nanowires. New Journal of Chemistry. 2016;**40**:5198-5208

[180] Lan J, Zhou X, Liu G, Yu J, Zhang J, Zhi L, et al. Enhancing photocatalytic activity of one-dimensional $KNbO_3$ nanowires by Au nanoparticles under ultraviolet and visible-light. Nanoscale. 2011;**3**:5161-5167

[181] Jiang L, Qui Y, Yi Z. Potassium niobate nanostructures: controllable morphology, growth mechanism, and photocatalytic activity. Journal of Materials Chemistry A. 2013;**1**:2878-2885

[182] Yan L, Zhang T, Lei W, Xu Q, Zhou X, Xu P, et al. Catalytic activity of gold nanoparticles supported on $KNbO_3$ microcubes. Catalysis Today. 2014;**224**:140-146

[183] Li G, Yi Z, Bai Y, Zhang W, Zhang H. Anisotropy in photocatalytic oxidization activity of $NaNbO_3$ photocatalyst. Dalton Transactions. 2012;**41**:10194-10198

[184] Hard template synthesis of nanocrystalline $NaNbO_3$ with enhanced photocatalytic performance. Catalysis Letters. 2012;**142**:901-906

[185] Katsumata K-I, Cordonier CEJ, Shichi T, FuJishima A. Photocatalytic activity of $NaNbO_3$ thin films. Journal of the American Chemical Society. 2009;**131**:3856-3857

[186] Yu J, Yu Y, Zhou P, Xiao W, Cheng B. Morphology-dependent photocatalytic-production activity of CDS. Applied Catalysis B. 2014:156-157

[187] Pai MR, Majeed J, Banerjee AM, Arya A, Bhattacharya S, Rao R, et al. Role of Nd3+ ions in modifying the band structure and photocatalytic properties of substituted indium titanates, $In_{2(1-x)}Nd_{2x}TiO_5$ oxides. Journal of Physical Chemistry C. 2012;**116**:1458-1471

[188] Haifeng S, Xiukai L, Hideol W, Zhingang Z, Jinhua Y. 3- Propanol photodegradation over nitrogen-doped $NaNbO_3$ powders under visible-light irradiation. Journal of Physics and Chemistry of Solids. 2009;**70**:931-935

[189] Paul B, Choo KH. Visible light active Ru-doped sodium niobate perovskite decorated with platinum nanoparticles via surface capping. Catalysis Today. 2014;**230**:138-144

[190] Shu H, Xie J, Xu H, Li H, Gu Z, Sun G, et al. Structural characterization and photocatalytic activity of NiO/$AgNbO_3$. Journal of Alloys and Compounds. 2010;**496**:633-637

[191] Li G, Kako T, Wamg D, Zou Z, Ye Y. Enhanced photocatalytic activity of La-doped $AgNbO_3$ under visible light irradiation. Dalton Transactions. 2009:2423-2427

[192] Wang Y, Gao Y, Chen L, Zhang H. Geothite as an efficient heterogeneous fenton catalyst for the degradation of methyl orange. Chemical Engineering Journal. 2012;**239**:322-331

[193] Li L, Zhang M, Tan P, Gu W, Wang X. Synthetic photocatalytic activity of $LnFeO_3$ (Ln=Pr, Y) perovskites under visible-light illumination. Ceramics International. 2014;**40**:13813-13817

[194] Jia L, Ding T, Li Q, Tang Y. Study of photocatalytic performance of $SrFeO_{3-x}$ by ultrasonic radiation. Catalysis Communications. 2007;**8**:963-966

[195] Gaffari M, Tan PY, Oruc ME, Tan OK, Tse MS. Effect of ball milling on the characteristics of nano structure $SrFeO_3$ powder for photocatalytic degradation of methylene blue under visible light irradiation and its reaction kinetics. Catalysis Today. 2011;**161**:70-77

[196] Ye T-N, Xu M, Fu W, Cai Y-Y, Wei X, Wang K-X, et al. The crystallinity effect of mesocrystalline $BaZrO_3$ hollow nanosheres on charge separation for photocatalysis. Chemical Communications. 2014;**50**:3021-3023

[197] Prastomo N, Zakaria NHB, Kawamura G, Muto H, Matsuda A. High surface area $BaZrO_3$ photocatalyst prepared by base-hot-water treatment. Journal of the European Ceramic Society. 2011;**31**:2699-2705

[198] Li L, Liu X, Zhang Y, Nuhfer NT, Barmak K, Salvador PA, et al. Visible-light photochemical activity of

heterostructured core–shell materials composed of selected ternary titanates and ferrites coated by TiO_2. ACS Applied Materials & Interfaces. 2013;**5**:5064-5071

[199] Cai Z, Zhou H, Song J, Zhao F, Li J. Preparation and characterization of $Zn_{0.9}Mg_{0.1}TiO_3$ via electrospinning. Dalton Transactions. 2011;**40**:8335-8339

[200] Wu G, Xiao L, Gu W, Shi W, Jiang D, Liu C. Fabrication and excellent visible-light-driven photodegradation activity for antibiotics of $SrTiO_3$ nanocube coated CdS microsphere heterojunctions. RSC Advances. 2016;**6**:19878-19886

[201] Wang Y, Niu C-G, Liang W, Wang Y, Zhang X-G, Zeng G-M. Synthesis of fern-like Ag/AgCl/$CaTiO_3$ plasmonic photocatalysts and their enhanced visible-light photocatalytic properties. RSC Advances. 2016;**6**:47873-47882

[202] Shu X, He J, Chen D. Visible-light-induced photocatalyst based on nickel titanate nanoparticles. Industrial and Engineering Chemistry Research. 2008;**47**:4750-4753

[203] Ding N, Chen X, Wu C-ML, Li H. Adsorption of nucleobase pairs on hexagonal boron nitride sheet: hydrogen bonding versus stacking. Physical Chemistry Chemical Physics. 2013;**15**:20203-20209

[204] Ma X, Zhang J, Li H, Duan B, Guo L, Que M, et al. Violet blue long-lasting phosphorescence properties of Mg-doped $BaZrO_3$ and its ability to assist photocatalysis. Journal of Alloys and Compounds. 2013;**580**:564-569

[205] Alammar T, Hamm I, Grasmik V, Wark M, Mudring A-V. Microwave-assisted synthesis of perovskite $SrSnO_3$ nanocrystals in ionic liquids for photocatalytic applications. Inorganic Chemistry. 2017;**56**(12):6920-6932

[206] Jung WY, Hong S-S. Synthesis of $LaCoO_3$ nanoparticles by microwave process and their photocatalytic activity under visible light irradiation. Journal of Industrial and Engineering Chemistry. 2013;**19**:157-160

[207] Dong B, Li Z, Li Z, Xu X, Song M, Zheng W, et al. Highly efficient $LaCoO_3$ nanofibers catalysts for photocatalytic degradation of rhodamine B. Journal of the American Ceramic Society. 2010;**93**:3587-3590

[208] Shasha F, Niu H, Tao Z, Song J, Mao C, Zhang S, et al. Low temperature synthesis and photocatalytic property of perovskite-type La-CoO_3 hollow spheres. Journal of Alloys and Compounds. 2013;**576**:5-12

[209] Lia Y, Yaoa S, Wenb W, Xuea L, Yana Y. Sol-gel combustion synthesis and visible-light-driven photocatalytic property of perovskite $LaNiO_3$. Journal of Alloys and Compounds. 2010;**491**:560-564

[210] Capon RJ, Rooney F, Murray LM, Collins E, Sim ATR, Rostas JAP, et al. Dragmacidins: New Protein Phosphatase Inhibitors from a Southern Australian Deep-Water Marine Sponge, Spongosorites sp. Materials Letters. 2007;**61**:3959-3962

[211] Hwang DW, Kim HG, Lee JS, Kim J, Li W, Se Hyuk O. Photocatalytic hydrogen production from water over M-Doped $La_2Ti_2O_7$ (M = Cr, Fe) under visible light irradiation ($\lambda > 420$ nm). The Journal of Physical Chemistry. B. 2005;**109**:15001-15007

[212] Hur SG, Kim TW, Hwang S-J, Choy J-H. Influences of A- and B-site cations on the physicochemical properties of perovskite-structured A(In1/3Nb1/3B1/3)O3 (A = Sr, Ba; B = Sn, Pb) photocatalysts. Journal of Photochemistry and Photobiology A. 2006;**183**:176-181

[213] Thirunavukkarasu SK, Abdul AR, Chidambaram J, Govindasamy R, Sampath M, Arivarasan VK, et al. Green synthesis of titanium dioxide nanoparticles using *Psidium guajava* extract and its antibacterial and antioxidant properties. Advances in Materials Research. 2014;**58**:968-976

[214] Aguiar R, Kalytta A, Reller A, Weidenkaff A, Ebbinghausc SG. Photocatalytic decomposition of acetone using LaTi(O,N)3 nanoparticles under visible light irradiation. Journal of Materials Chemistry. 2008;**18**:4260-4265

[215] Wang D, Kako T, Ye J. Efficient photocatalytic decomposition of acetaldehyde over a solid-solution perovskite $(Ag_{0.75}Sr_{0.25})(Nb_{0.75}Ti_{0.25})O_3$ under visible-light irradiation. Journal of the American Chemical Society. 2008;**130**:2724-2725

[216] Dong W, Kaibin T, Zhenhua L, Huagui Z. Synthesis, crystal structure, and photocatalytic activity of the new three-layer aurivillius phases, $Bi_2ASrTi_2TaO_{12}$ (A = Bi, La). Journal of Solid State Chemistry. 2010;**183**:361-366

[217] Fanke M, Zhanglian H, James A, Ming L, Mingjia Z, Feng Y, et al. Visible light photocatalytic activity of nitrogen-doped $La_2Ti_2O_7$ nanosheets originating from band gap narrowing. Nano Research. 2012;**5**:213-221

[218] Danjun W, Huidong S, Li G, Feng F, Yucang L. Design and construction of the sandwich-like z-scheme multicomponent cds/ag/bi2moo6 heterostructure with enhanced photocatalytic performance in rhb photodegradation. New Journal of Chemistry. 2016;**40**:8614-8624